IJST (2015) 39A3 (Special issue): 445-453
Iranian Journal of Science & Technology

http://ijsts.shirazu.ac.ir

Study the heat dissipation performance of horizontal battery pack

X. Xiaoming*, T. Wei, J. Haobin and G. Ran

School of Automotive and Traffic Engineering, Jiangsu University, Zhenjiang, China, 212013
E-mail: xuxiaoming3777@163.com

Abstract

Battery pack is the main energy storage element, and directly affects the performance of electric vehicle. This paper selects the forced air cooling of horizontal battery pack as the study object, and researches the heat dissipation performance of different operating conditions with FLEUNT software. Results indicate that: according to the four kinds of transient state conditions and steady state condition, the temperature rising of horizontal battery pack is significantly higher than the temperature difference; when the electric vehicle beginning to decrease speed, the curve of temperature rising and temperature difference rise, it shows that the internal heat continuously rising up, so even the electric vehicle beginning to decrease speed, the fan must work. Then the reference basis for heat flow field characteristic analysis of horizontal battery pack is offered.

Keywords: Electric vehicle; heat dissipation performance; battery pack; operation conditions; transient state; steady state; temperature rising; temperature difference

1. Introduction

Forced air cooling is widely used as the cooling method of battery pack at home and abroad, many researchers have carried out the related work. For battery pack arrangement (Rami et al., 2008; Tassou et al., 2010; Xu et al., 2014), the forced air cooling was separated into serial airflow and parallel airflow (Takak et al., 1998); the forced air cooling system developed by Toyota corporation was the most representative, and the relevant patents were applied (Osamu and Kanagawa, 2003); the heat dissipation performance of Hybrid-Electric vehicle battery pack was researched by software STAR-CD and ANSYS, and validated by experiments (Pan et al., 2005); the thermal management system of Ni-MH battery pack was researched (Fu et al., 2005); the thermal management system of electric vehicle battery pack was researched, and the cooling system structure design of Toyota RAV-4 electric vehicle was analyzed (Zhu,2007); when the speed of electric vehicle was constant, the temperature field of lithium-ion battery pack based on natural air cooling was researched by simulation and experiment (Liu et al., 2012). In addition, there are many forced air cooling systems of battery pack developed by researchers and manufacturers, in order to improve the temperature distribution uniformity of battery module (Kiziel et al., 2008; Nielsen et al., 2012; Xu et al., 2013; Xu et al., 2013).

This paper selects the forced air cooling of horizontal battery pack (as shown in Fig. 1, the air-inlets are on the opposite position of fans, and both sides of horizontal battery pack; the battery pack has a total of 48 batteries, and includes 4 battery modules with 2 parallels and 6 series) as the study subject, and researches the heat dissipation performance of different operating conditions (including steady state and transient state), in order to offer a reference basis for heat flow field characteristic analysis of horizontal battery pack.

2. Thermal power determination test of 55ah lithium-ion battery on charge and discharge processing

2.1. Thermal physical parameters of 55Ah lithium-ion battery

Table 1 shows the thermal physical parameters of 55Ah lithium-ion battery: the density of electric core is 2123 $kg(m^3)^{-1}$, the thermal conductivity coefficient is 30.6 $W(m\cdot K)^{-1}$, and the specific heat capacity is 913 $J(kg\cdot K)^{-1}$.

*Corresponding author
Received: 28 July 2013 / Accepted: 5 July 2015

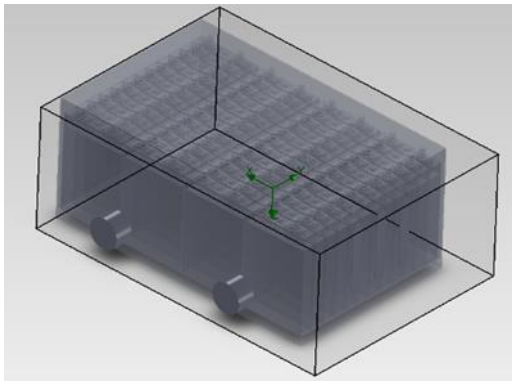

Fig. 1. Horizontal battery pack

Table 1. Thermal physical parameters of 55Ah lithium-ion battery

Battery component	Density（kg(m^3)$^{-1}$）	Thermal conductivity coefficient (W(m·K)$^{-1}$)	Specific heat capacity（J(kg·K)$^{-1}$）
electric core	2123	30.6	913
the positive pole	2719	202.4	871
the negative pole	8978	387.6	381
the diaphragm	1008	0.3344	1978
shell	8193	14.7	439.3

2.2. Thermal power determination test of 55Ah lithium-ion battery on charge and discharge processing

Figure 2 shows the arrangement of temperature measuring point and the design of thermal insulation with 55Ah lithium-ion battery, including 2 measuring points on bottom and 3 measuring points on side wall, heat insulation box has three layers of insulating material surround, to ensure good thermal insulation performance.

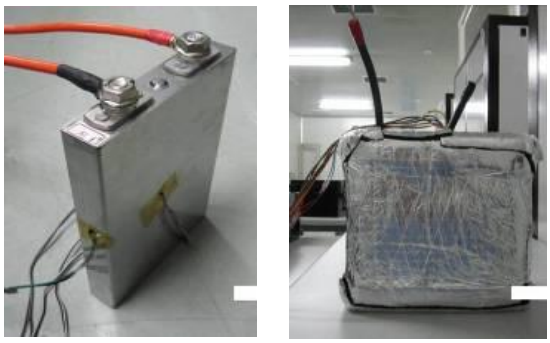

Fig. 2. The arrangement of temperature measuring point and the design of thermal insulation with 55Ah lithium-ion battery, (a) Temperature measuring point (b) Heat insulation box

Calorific value calculation formula is as follows:

$$Q = c_p m \Delta T \tag{1}$$

Q means calorific value; c_p means specific heat capacity; m means quality; ΔT means temperature rise.

It could be introduced into the thermal power calculation formula by formula (1) as follows:

$$P = \frac{c_p m \Delta T}{t} \tag{2}$$

P means thermal power; t means time.

Constant temperature box is set at 20℃, the experimental processing is as follows: firstly, setting a certain charge rate up to 3.65V; secondly, turning to constant-voltage charge, until 0.05C cutoff; thirdly, setting this discharge rate down to 2.50V.

When the temperature is 20℃, Fig 3 shows the average temperature curves of 55Ah lithium-ion battery monomer at 0.5C charge and discharge rate, Table 2 shows the temperature data at different charge and discharge rates, as could be seen from Table3, the average thermal power of 55Ah lithium-ion battery monomer is 2.31W at 0.5C, 3.42W at 0.6C, 5.00W at 0.8C, 6.51W at 1C, 8.44W at 1.2C, 12.83W at 1.5C, and 19.17W at 2C, it is obvious that the average thermal power of 55Ah lithium-ion battery monomer increase along with charge and rising discharge rate.

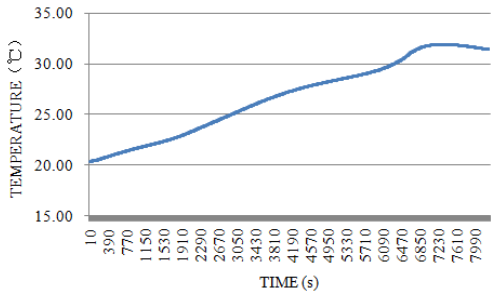

(a) Charge processing

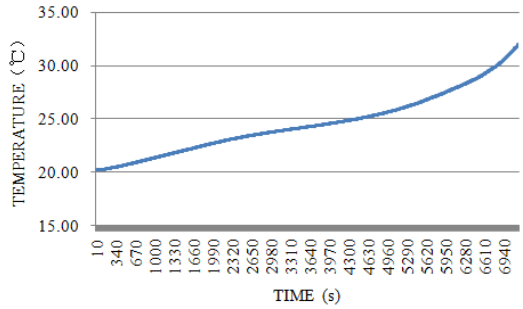

(b) Discharge processing

Fig. 3. The average temperature curve of 55Ah lithium-ion battery monomer at 0.5C charge and discharge rate

Table 2. The temperature data of 55Ah lithium-ion battery monomer at different charge and discharge rates（℃）

Charge and discharge rate	Starting temperature		Final temperature		Total temperature rising	
	charge	discharge	charge	discharge	charge	discharge
0.5C	20.39	20.19	31.40	32.01	11.01	11.82
0.6C	20.33	20.21	34.03	35.23	13.70	15.02
0.8C	20.20	20.25	35.54	36.75	15.34	16.50
1C	19.92	20.05	35.43	37.39	15.51	17.34
1.2C	20.11	20.11	37.25	39.92	17.14	19.81
1.5C	20.22	20.37	43.16	44.49	22.94	24.12
2C	20.27	20.29	45.39	47.99	25.12	27.70

Table 3. The thermal power of 55Ah lithium-ion battery at different charge and discharge rates（W）

Charge and discharge rate	Average thermal power on charge processing	Average thermal power on discharge processing	Average thermal power on charge and discharge processing
0.5C	2.06	2.55	2.31
0.6C	2.95	3.89	3.42
0.8C	4.31	5.69	5.00
1C	5.42	7.60	6.51
1.2C	6.62	10.25	8.44
1.5C	10.06	15.60	12.83
2C	14.44	23.89	19.17

3. Calculation method and boundary condition

3.1. Mathematical model

Normally, the maximum velocity of airflow in battery pack is less than 400km/h, it means less than 1/3 sound velocity, so the airflow in battery pack could be considered in incompressible flow, and the physical parameters of airflow are constant number. Combined with the phenomenon of air separation by complex structure of battery pack, turbulent processing should be considered. The control equations are as follows:

Continuity equation:

$$\nabla \cdot \bar{v} = 0 \tag{3}$$

Momentum conservation equation:

$$\frac{\partial \bar{v}}{\partial t} + (\bar{v} \cdot \nabla)\bar{v} = -\frac{\nabla p}{\rho} + \frac{\mu}{\rho}\nabla^2 \bar{v} \tag{4}$$

Energy conservation equation:

$$\rho \cdot c_p \cdot \left(\frac{\partial \mathrm{E}}{\partial t} + u \cdot \frac{\partial \mathrm{E}}{\partial x} + v \cdot \frac{\partial \mathrm{E}}{\partial y} + w \cdot \frac{\partial \mathrm{E}}{\partial z} \right) = \lambda \cdot \left(\frac{\partial^2 \mathrm{E}}{\partial x^2} + \frac{\partial^2 \mathrm{E}}{\partial y^2} + \frac{\partial^2 \mathrm{E}}{\partial z^2} \right) \tag{5}$$

$\bar{v}$ means velocity vector, t means time, p means pressure, ρ means density, μ means viscosity coefficient, c_p means specific heat, E means total energy, u、v and w mean the velocity of x、y and z direction, λ means thermal conductivity coefficient.

3.2. Calculation method

Three-dimensional incompressible Navier-Stokes equations and Standard $k-\varepsilon$ model are used in simulation, and SIMPLEC method is iterated.

3.3. Boundary condition

The air-inlet is free inlet boundary condition, and the pressure is standard atmospheric pressure. The air-outlet is fan outlet boundary condition, and Fig. 4 shows the curve between fan pressure difference and flow rate: when the pressure difference between air-inlet and air-outlet is 125Pa, the flow rate is 0.0028 m^3/s (10.8 m^3/h); when the pressure difference between air-inlet and air-outlet is 0Pa, the flow rate is 0.0083 m^3/s (29.9 m^3/h), the battery pack includes two fans. No-slip boundary condition is used as wall surface, and the speed is zero. The heat power of lithium-ion battery depends on the given specific example.

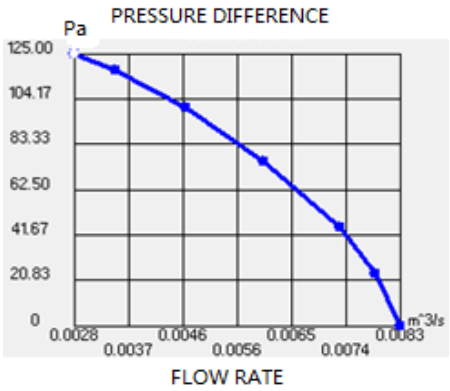

Fig. 4. The curve between pressure difference and flow rate

3.4. Heat dissipation performance indexes

Assessing the heat dissipation performance of battery pack cooling system has two main indexes: the rising maximum temperature and temperature difference (it defines the maximum difference value between battery pack maximum temperature and environmental temperature as maximum temperature rise, and the maximum value of battery pack internal temperature difference as maximum temperature difference). If the rise the maximum temperature is too big, it means the environment temperature is relatively poor for the battery pack to work, and the heat generated by battery pack could not be effectively removed through the cooling system; if the maximum temperature difference is too big, it means the temperature distribution uniformity of battery pack is poor, so the purpose of battery pack cooling system design should be set to reduce the maximum temperature rise and temperature difference.

4. Calculation and analysis

4.1. Steady state calculation

When the environment temperature is 20℃, Fig. 5 shows the temperature field and velocity trace of horizontal battery pack with steady state calculation. It could be seen from Fig. 5 (a) that the high temperature area of horizontal battery pack is in the center, and the temperature of air-inlet is relatively low. Airflow is inhaled from the air-inlet, and heated by battery pack, so airflow temperature rises and, eventually leads the airflow cooling capacity to decrease. As could be seen from Fig. 5 (b), the distribution of airflow velocity trace is more uniform, which is conducive to the airflow cooling. The maximum temperature rise and maximum temperature difference of horizontal battery pack are 15.89℃ and 9.75℃, and the difference value between them is 6.14℃.

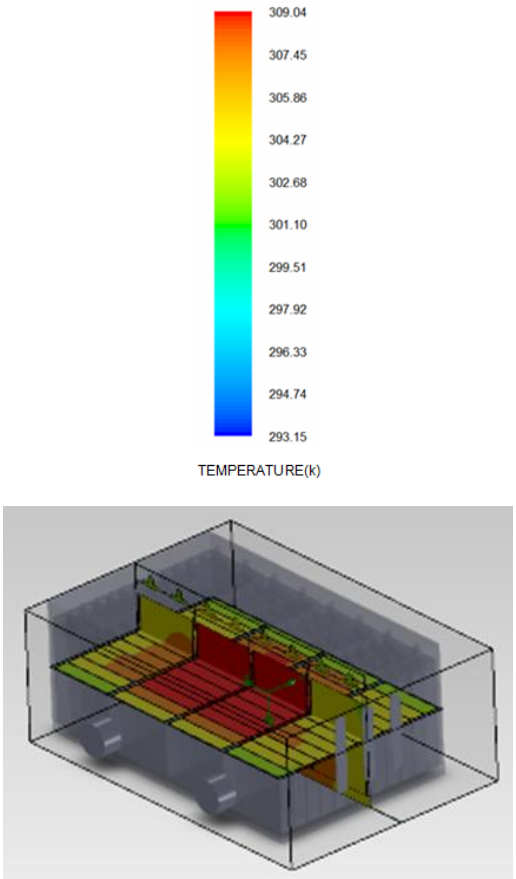

(a) Temperature field

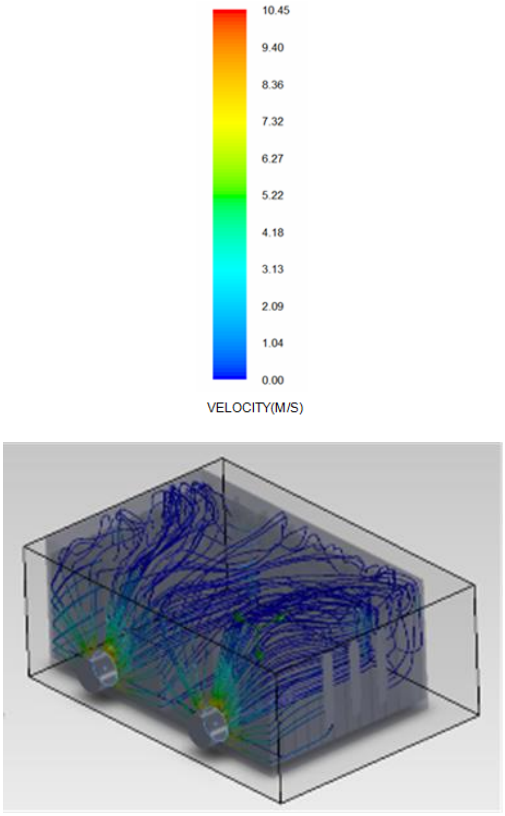

(b) Velocity trace

Fig. 5. The temperature field and velocity trace of horizontal battery pack with steady state calculation

4.2. Sustained acceleration

When the environment temperature is 20℃, Table4 shows the operating condition of electric vehicle sustained acceleration: firstly, the constant current discharge processing with 0.6C is 10 minutes; secondly, the constant current discharge processing with 0.8C is 5 minutes; thirdly, the constant current discharge processing with 1C is 2 minutes; finally, the constant current discharge processing with 1.5C is 1 minute; so the time of total discharge processing is 18 minutes, and no intermediate pause.

Table 4. The operating condition of electric vehicle sustained acceleration

serial number	operating state	discharge rate	time（minute）
1	constant current discharge	0.6C	10
2	constant current discharge	0.8C	5
3	constant current discharge	1C	2
4	constant current discharge	1.5C	1

Figure 6 shows the temperature field and velocity trace of horizontal battery pack at the end time of electric vehicle sustained acceleration, as can be seen, the temperature distribution of horizontal battery pack is uniform with transient state calculation, this is because the heat in battery pack has not been fully released by airflow, the velocity trace is close to steady state calculation. Figure 7 shows rising temperature curves and inner temperature difference following the electric vehicle sustained acceleration. When the discharge rate increases from 0.6C to 1.5C, the thermal power of horizontal battery pack rises, and the curve slope of temperature rise and inner temperature difference increases, too; moreover, the rising temperature of horizontal battery pack is evidently higher than the inner temperature difference. At the end of electric vehicle sustained acceleration, the maximum temperature rise of horizontal battery pack is 3.71℃, and the maximum temperature difference of horizontal battery pack is 2.10℃, the difference value between them is 1.61℃.

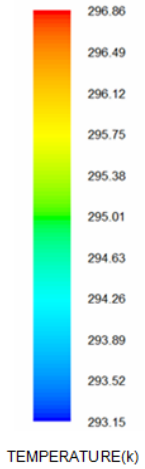

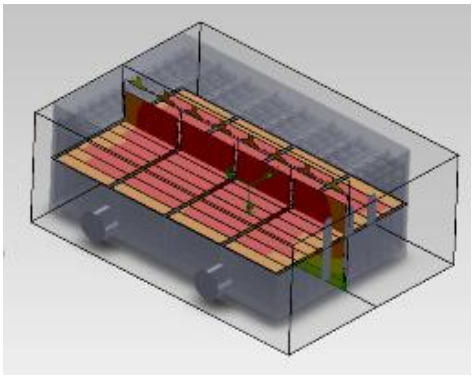

(a) Temperature field

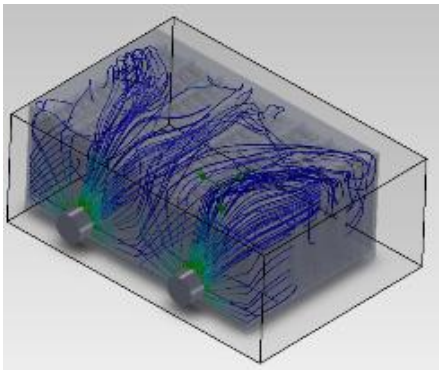

(b) Velocity trace

Fig. 6. At the end of electric vehicle sustained acceleration, the temperature field and velocity trace of horizontal battery pack

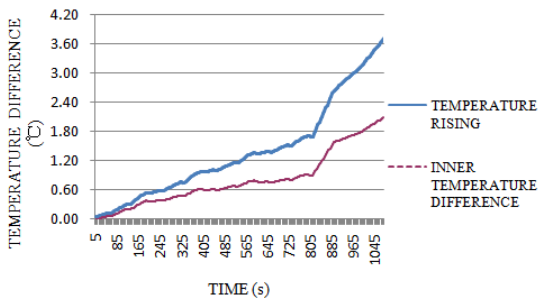

Fig. 7. The rising of temperature curves and inner temperature difference following the sustained electric vehicle acceleration

4.3. Sustained deceleration

When the temperature is 20℃, Table5 shows the operating condition of electric vehicle sustained deceleration: firstly, the constant current discharge processing with 2C is 0.5 minute; secondly, the constant current discharge processed at 1.5C is 1 minute; thirdly, the constant current discharge processed at 1.2C is 2 minutes; fourthly, the constant current discharge processed at 1C is 5 minutes; fifthly, the constant current discharge processed at 0.8C is 8 minutes; finally, the constant current discharge processed at 0.5C is 12 minutes; so the time of total discharge processing is 28.5 minutes, and no intermediate pause.

Table 5. The operating condition of electric vehicle sustained deceleration

Serial number	Operating state	Discharge rate	Time （minute）
1	constant current discharge	2C	0.5
2	constant current discharge	1.5C	1
3	constant current discharge	1.2C	2
4	constant current discharge	1C	5
5	constant current discharge	0.8C	8
6	constant current discharge	0.5C	12

Figure 8 shows the rising temperature curves and inner temperature difference following the electric vehicle sustained deceleration. When the discharge rate decreases from 2C to 0.5C, the thermal power of horizontal battery pack falls, but considering the superposition effect of temperature, the heat in battery pack could not be released quickly by airflow, so the temperature rising curves and inner temperature difference still rise, while the curve slope is on the decline; the temperature rising curves and inner temperature difference rise along with electric vehicle sustained acceleration, therefore, even if the electric vehicle begins to decelerate, the fan must work until the temperature of battery pack decreases. At the end of electric vehicle sustained deceleration, the maximum temperature risie of horizontal battery pack is 5.09℃, and the maximum temperature difference of horizontal battery pack is 3.02℃, the difference value between them is 2.07℃.

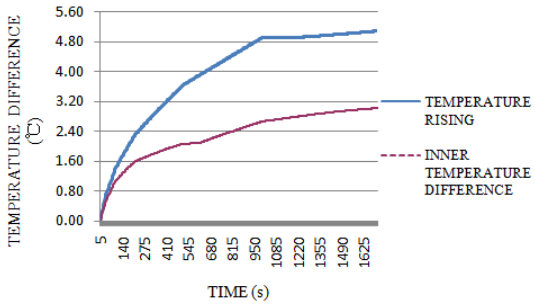

Fig. 8. The curves of temperature rising and inner temperature difference following the electric vehicle sustained deceleration

4.4. Pause and pulse discharge processing

When the environment temperature is 20℃, Table6 shows the operating condition of pause and pulse discharge processing, it consists four basic operating conditions of 1 and one basic operating condition of 2, so the time of total discharge processing is 1200 seconds.

Table 6. The operating condition of pause and pulse discharge processing

Stage	Serial number	Operating state	Discharge rate	Time（second）
Basic operating condition of 1	1	pause	0	10
	2	constant current discharge	0.5C	30
	3	pause	0	15
	4	constant current discharge	0.6C	60
	5	pause	0	15
	6	constant current discharge	0.8C	40
	7	constant current discharge	0.6C	20
	8	pause	0	10
Basic operating condition of 2	1	pause	0	10
	2	constant current discharge	1.5C	80
	3	constant current discharge	1C	100
	4	constant current discharge	1.2C	80
	5	constant current discharge	1.5C	80
	6	constant current discharge	2C	40
	7	pause	0	10

Because the thermal power of horizontal battery pack is not continuous on the processing of pause and pulse discharge, as could be seen from Fig. 9 the rising temperature curves and inner temperature difference of horizontal battery pack are not smooth and continuous. On the four basic operating conditions of 1, the discharge rate of horizontal battery pack is relatively low, so the rising temperature curves and inner temperature difference of horizontal battery pack are relatively flat; On the one basic operating condition of 2, the discharge rate of horizontal battery pack is relatively high, so the curves shoeing the rise in temperature and inner temperature difference of horizontal battery pack are relatively steep. The temperature rise of horizontal battery pack is evidently higher than the inner temperature difference too, at the end of the processing of pause and pulse discharge, the maximum temperature rising of horizontal battery pack is 5.19℃, and the maximum temperature difference of horizontal battery pack is 3.01℃, the difference value between them is 2.18℃.

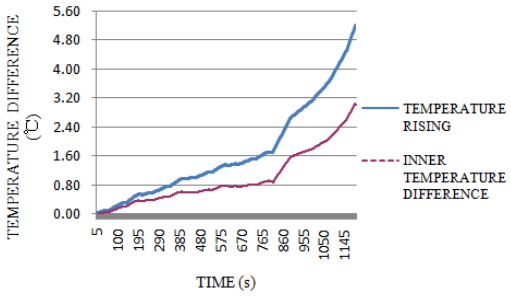

Fig. 9. The curves of temperature rising and inner temperature difference with the operating condition of pause and pulse discharge processing

4.5. Heat dissipation performance analysis with practical operation condition

Figure 10 shows the curve of electric current following the battery pack work (battery pack work time is 3000s), taking into consideration the practical operation condition of battery pack is very complicated, As could be seen from Table 7, based on the practical operation of battery pack, the average charge rate is 0.51C, and the average heat

power of lithium-ion battery is 2.06W; the average discharge rate is 0.80C, and the average heat power of lithium-ion battery is 5.69W.

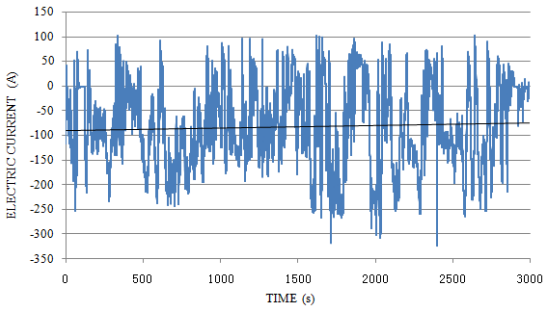

Fig. 10. The curve of electric current following the battery pack work

Table 7. Practical operation condition of battery pack

	charge processing	discharge processing
the average electric current (A)	56.05	87.88
time（S)	513	2487
charge and discharge rate	0.51C	0.80C
the average heat power（W）	2.06	5.69

When the environmental temperature is 20℃, Fig. 11 shows the curve of temperature rising and temperature difference following the battery pack practical work, it could be seen that the maximum temperature rising of horizontal battery pack is 7.61℃, and the maximum temperature difference of horizontal battery pack is 4.29℃, the difference value between them is 3.32℃.

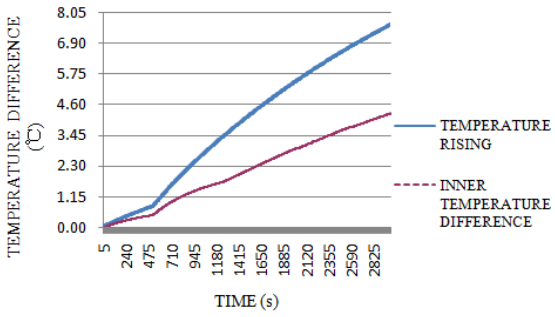

Fig. 11. The rising temperature curve and inner temperature difference following the battery pack practical work

5. Conclusions

Through the above research, the conclusions are as follows:

(1) Steady state calculation: the high temperature area of horizontal battery pack is in the center, and the temperature of air-inlet is relatively low; the distribution of airflow velocity trace is more uniform, which is conducive to the airflow cooling.

(2) The transient state calculation include: sustained acceleration, sustained deceleration, pause and pulse discharge processing, practical operation condition. At the end of all the transient states, the maximum temperature rise of horizontal battery pack is higher than the maximum temperature difference.

(3) The rising temperature curves and increase in inner temperature difference along with electric vehicle sustained acceleration, therefore, even if the electric vehicle begins to decelerate, the fan must work until the battery pack temperature decreases.

Acknowledgment

This work was supported by National Natural Science Foundation of China(51505196), Jiangsu Provincial Natural Science Foundation of China (BK20140559), China Postdoctoral Science Foundation (2014M561582), Jiangsu Province Postdoctoral Science Foundation(1302036B), Foundation of Jiangsu University(1281120041).

References

Fu, Z. Y., Lin, C. T., & Chen, Q. S. (2005). Key technologies of thermal management system for EV battery packs. *Journal of Highway and Transportation Research and Development*, 22(3), 119–123.

Kiziel, R., Lateef, A., Farid, M. M., & et al. (2008). Passive control of temperature excursion and uniformity in high–energy Li–ion battery packs at high current and ambient temperature. *Journal of Power Sources*, 183, 370–375.

Liu, Z. J., Lin, G. F., Qin, D. T., & et al. (2012). A study on the temperature field of lithium-ion battery pack in an electric vehicle and its structural optimization. *Automotive Engineering*, 34(1), 80–84.

Nielsen, K. K., Engelbrecht, K., & Christensen D. V. (2012). Degradation of the performance of micro channel heat exchangers due to flow misdistribution. *Applied Thermal Engineering*, 40, 236–247.

Osamu, W., & Kanagawa. (2003). Battery cooling structure. US: 06613472, Tokyo R & D Co.

Pan, H. B., Zhao, J. H., Feng, X. Z., & et al. (2005). Use of simulation technology on the construction design of nickel hydride metal piles. *Chinese Journal of Mechanical Engineering*, 41(12), 58–61.

Rami, S., Kizilel, R., Selman, J. R., & et al. (2008). Active (air–cooled) vs passive (phase change material) thermal management of high power lithium–ion packs: limitation of temperature rise and uniformity of temperature distribution. *Journal of Power Sources*, 182, 630–638.

Takak, A. i., Toyoaki, N., Hideaki, H., & et al. (1998). Development of a high-power battery cooling system for series HEVs. Belgium, Brussels, EVS–15.

Tassou, S. A., Lewis, J. S., & Ge, Y. T. (2010). A review

of emerging technologies for food refrigeration applications. *Applied Thermal Engineering*, 30, 263–276.

Xu, L. F., Ouyang, M. G., Li, J. Q., & et al. (2013). Application of pontryagin's minimal principle to the energy management strategy of plugin fuel cell electric vehicles. *Int J Hydrogen Energy*, 38(24), 10104–15.

Xu, L. F., Li, J. Q., Ouyang, M. G., & et al. (2014). Multi–mode control strategy for fuel cell electric vehicles regarding fuel economy and durability. *Int J Hydrogen Energy*, 39(5), 2374–89.

Xu, X. M., & He, R. (2013). Research on the heat dissipation performance of battery pack based on forced air cooling. *Journal of Power Sources*, 240, 33–41.

Zhu, X. T. (2007). Study in wind cooling system for RAV–4 EV packs. Nanjing, China: Nanjing University of Aeronautics and Astronautics.